Open access • Journal Article • DOI:10.2514/3.470

Variable Refractive Index Effects on Radiation in Semitransparent Scattering Multilayered Regions — Source link

Robert Siegel, Charles M. Spuckler

Institutions: Glenn Research Center

Published on: 01 Oct 1993 - Journal of Thermophysics and Heat Transfer (American Institute of Aeronautics and Astronautics (AIAA))

Topics: Step-index profile, Optical properties of water and ice, Total internal reflection, Radiative transfer and Heat transfer

E-9815

Variable Refractive Index Effects on Radiation in Semitransparent Scattering Multilayered Regions

R. Siegel and C. M. Spuckler

Reprinted from

Journal of Thermophysics and Heat Transfer

Volume 7, Number 4, October–December 1993, Pages 624–630

AIAA

A publication of the
American Institute of Aeronautics and Astronautics, Inc.
The Aerospace Center, 370 L'Enfant Promenade, SW
Washington, DC 20024-2518

JOURNAL OF THERMOPHYSICS AND HEAT TRANSFER
Vol. 7, No. 4, Oct.–Dec. 1993

Variable Refractive Index Effects on Radiation in Semitransparent Scattering Multilayered Regions

R. Siegel* and C. M. Spuckler†
NASA Lewis Research Center, Cleveland, Ohio 44135

A simple set of equations is derived for predicting the temperature distribution and radiative energy flow in a semitransparent layer consisting of an arbitrary number of laminated sublayers that absorb, emit, and scatter radiation. Each sublayer can have a different refractive index and optical thickness. The plane composite region is heated on each exterior side by a different amount of incident radiation. The results are for the limiting case where heat conduction within the layers is very small relative to radiative transfer, and is neglected. The interfaces are assumed diffuse, and all interface reflections are included in the analysis. The thermal behavior is readily calculated from the analytical expressions that are obtained. By using many sublayers, the analytical expressions provide the temperature distribution and heat flow for a diffusing medium with a continuously varying refractive index, including internal reflection effects caused by refractive index gradients. Temperature and heat flux results are given to show the effect of variations in refractive index and optical thickness through the multilayer laminate.

Nomenclature

a_j = absorption coefficient of jth sublayer, m^{-1}
D = total thickness of the composite plane layer, m
D_j = thickness of jth sublayer in composite, m
E_1, E_2, E_3 = exponential integral functions, $E_m(x) = \int_0^1 \mu^{m-2} \exp(-x/\mu)\, d\mu$
$F(n)$ = function of refractive index defined in Eq. (19a)
n_j = index of refraction of jth sublayer
q = heat flux, W/m^2
q^o_{r1}, q^o_{r2} = externally incident radiative flux, W/m^2
$\bar{q}_r$ = dimensionless radiative heat flux, $q_r/(q^o_{r1} - q^o_{r2})$
R_j = quantity $\rho_j^i/(1 - \rho_j^i)$
T = absolute temperature, K
$\bar{T}^4$ = dimensionless temperature function, $(\sigma T^4 - q^o_{r2})/(q^o_{r1} - q^o_{r2})$
X_j = dimensionless local coordinate in jth sublayer, x_j/D_j
x = coordinate normal to boundaries of composite plane region, m; x_j, local coordinate in jth sublayer, m
κ_D = optical thickness of entire layer $\kappa_1 + \kappa_2 + \cdots + \kappa_J$; κ_{Dj} optical thickness of the jth sublayer $(a_j + \sigma_{sj})D_j$
κ_j = optical depth in a sublayer $(a_j + \sigma_{sj})x_j$; extinction coefficient in the complex index of refraction
λ_0 = radiation wavelength in vacuum
ρ^i, ρ^o = reflectivity of interface for internally and externally incident radiation
σ = Stefan-Boltzmann constant, $W/(m^2 \cdot K^4)$
σ_{sj} = scattering coefficient in jth sublayer, m^{-1}
τ^i, τ^o = transmissivity of interface for internally and externally incident radiation
Φ = dimensionless temperature function, Eq. (3)
Ψ = dimensionless radiative heat flux function, Eq. (4)

Subscripts
f, s = first ($x_j = 0$) and second ($x_j = D_j$) internal interfaces of a sublayer within the composite
H, L = higher and lower values
i, o = incoming and outgoing radiation
J = total number of sublayers in the composite
j = jth sublayer in the multilayer composite, $1 \le j \le J$
r = radiative quantity

Superscripts
i = inside surface of an interface
o = outside surface of an interface

Introduction

THE use of ceramic parts or coatings is of interest for high-temperature applications. Some parts may have reinforcing layers or may be laminated, so it is necessary to consider heat transfer in composite materials. Surrounding temperatures are usually high, so there can be appreciable heating by radiation. Since some ceramics are semitransparent, their temperature distributions are influenced by internal radiative heat flow. The refractive indices of the sublayers in a composite can have a considerable effect on the temperature distribution and radiative heat flow. Surface reflections depend on the refractive indices on both sides of the interface, so the refractive indices influence both the external energy transmitted into the interior of a material and the amount of internal energy reflected back into the interior. Within a material, emission depends on its refractive index squared; hence, internal emission can be many times that for a blackbody radiating into a vacuum. Since internal radiation exiting through an interface into a vacuum cannot exceed that of a blackbody, there can be considerable reflection at the internal surface of an interface, partially by total internal reflection. If there is a gradient of refractive index in the material, it will cause some of the radiation to be refracted backward when initially directed into a region with a smaller refractive index. These effects distribute internal energy within the material and make

Received Sept. 4, 1992; revision received Nov. 23, 1992; accepted for publication Nov. 24, 1992.

*Research Scientist, Lewis Research Academy. Fellow AIAA.
†Research Scientist, Heat Transfer Branch.

the temperature distribution more uniform than in a region with a refractive index close to unity. This article will provide some insight into these effects by examining the limiting case where heat transfer is only by radiation.

In Siegel and Spuckler[1,2] it was shown that for radiative equilibrium (no conduction or convection) in a single- or two-layer gray medium with diffuse interfaces, the temperature distribution and radiative heat flux for any refractive index can be readily obtained from available results for a single layer with a refractive index of one. This article uses these ideas extended to a multilayer laminate to determine radiative transfer characteristics in a layer with a continuous variation of refractive index. Analytical expressions that are readily evaluated are obtained for the temperature distribution and radiative heat flow. Each sublayer emits, absorbs, and isotropically scatters radiation. For simplicity, the external medium on each side of the entire laminate has a refractive index of one.

The outer surfaces of the laminate, and all interfaces between adjacent layers, are assumed diffuse. This is probably a reasonable approximation for ceramics that have not been polished and are bonded together. When transmitted radiation, or radiation emitted from the interior, reaches the inner surface of an interface, it is assumed diffuse as a result of scattering within the medium. If the index of refraction of the material is greater than that of the surrounding medium, some of this diffuse energy is in angular directions for which there is total internal reflection. These reflections provide a trapping effect that retains energy within the layer with the larger refractive index, and tends to equalize the local temperature distribution in this layer.

There have been many studies of radiative transfer in semitransparent layers. However, very little has been done to examine the effects of a variable refractive index, especially with regard to computing internal temperature distributions when there is internal emission and scattering. To predict heat treating and cooling of glass plates, Gardon[3] developed an analysis for temperature distributions in absorbing-emitting layers, including uniform refractive index effects. The interfaces were optically smooth, and specular reflections at the interfaces were computed from the Fresnel reflection relations. A similar application, Fowle et al.,[4] predicted heating in a window of a re-entry vehicle. Some recent papers[5-8] further examined the effects of Fresnel boundary reflections and a nonunity uniform refractive index. Many analyses of both steady and transient heat transfer to single or multiple plane layers, such as Amlin and Korpela[9] and Tarshis et al.,[10] have used diffuse conditions at the interfaces as in the present study. Thomas[11] set up a solution procedure to include a ceramic interface that is partially specular and diffuse. Ritchie and Window[12] and Snail[13] analyzed the reflection behavior of thin films with a graded refractive index. The results are concerned with the effect of thin films on the absorption of solar radiation and do not consider their internal temperature distribution.

Analysis

A laminated plane layer consists of an arbitrary number of J sublayers of different materials with thicknesses $D_1, D_2, \ldots, D_j, \ldots, D_J$, as in Fig. 1a. Each sublayer absorbs, emits, and isotropically scatters radiation. The limiting case is examined here where energy transfer within the laminated region is dominated by radiation, so heat conduction is neglected (in the literature this limit is referred to as "radiative equilibrium"). An analytical solution is obtained which can provide a helpful basic limiting case for numerical studies in which conduction is included. Each sublayer has a constant n_j; it is the effect of the different refractive indices and the different optical thicknesses of the sublayers that is investigated here. The materials are assumed to provide significant scattering, so the energy fluxes are assumed diffuse at the

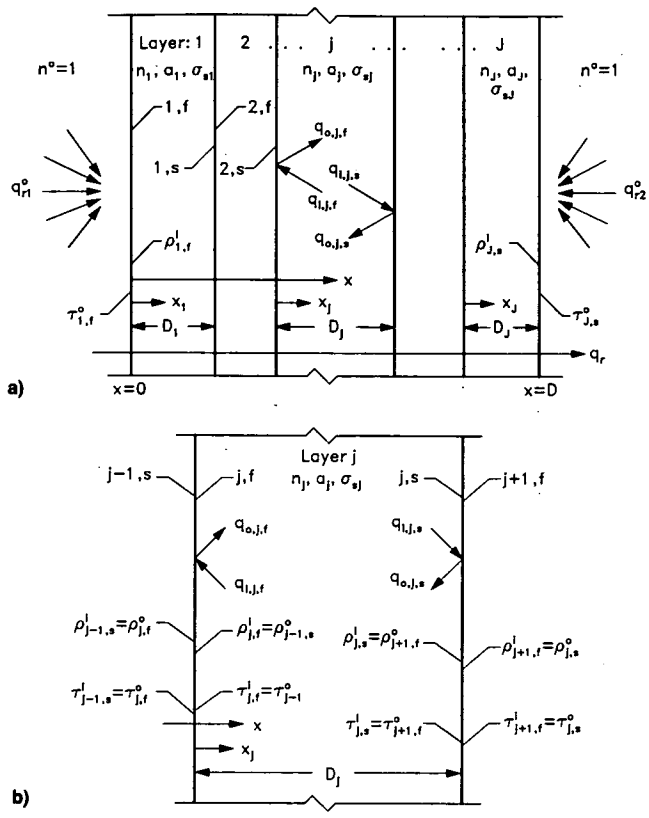

Fig. 1 Laminated multilayer geometry: a) coordinate systems in layers, and nomenclature designating interfaces and their heat fluxes; b) detailed nomenclature for the jth layer.

interfaces between sublayers and between the outer sublayers and the surrounding air or vacuum. For simplicity, the refractive index of the surroundings is one.

As shown in Fig. 1a the laminated region is subjected to diffuse q^o_{r1} and q^o_{r2} from the external surroundings onto the two outer boundaries $x_1 = 0$ and $x_J = D_J$; for convenience $q^o_{r1} > q^o_{r2}$. Within each sublayer, the analysis will use outgoing and incoming fluxes, $q_{o,j}$ and $q_{i,j}$, that are moving away from or toward each interior interface of each sublayer. Since scattering is included, the local optical depth within each sublayer is related to its individual x_j coordinate by $\kappa_j = (a_j + \sigma_{sj})x_j = (a_j + \sigma_{sj})D_jX_j = \kappa_{Dj}X_j$.

The temperature distribution in each sublayer is governed by an integral equation (Siegel and Howell[14]) with index of refraction factors included to give for the jth sublayer

$$n_j^2\sigma T_j^4(X_j, \kappa_{Dj}) = \frac{1}{2}\{q_{o,j,f}E_2(\kappa_{Dj}X_j) + q_{o,j,s}E_2[\kappa_{Dj}(1 - X_j)]\} + \frac{n_j^2}{2}\kappa_{Dj}\int_0^1 \sigma T_j^4(X_j^*)E_1(\kappa_{Dj}|X_j - X_j^*|)\,dX_j^* \quad (1)$$

where $q_{o,j,f}$ and $q_{o,j,s}$ are the outgoing internal radiative fluxes from the first and second interfaces of the jth layer as shown in Fig. 1. The energy equation $dq_r/dx = 0$ shows that q_r being transferred through the entire laminated layer is *constant* for the present conditions of radiative equilibrium (negligible internal heat conduction). The relation of q_r to the temperature distribution in any of the sublayers is obtained by using the expression for q_r within a plane layer as given in Ref. 14. This is evaluated at $x = 0$ to give for the jth sublayer

$$q_r(\kappa_{Dj}) = q_{o,j,f} - 2q_{o,j,s}E_3(\kappa_{Dj}) - 2n_j^2\kappa_{Dj}\int_0^1 \sigma T_j^4(X_j)E_2(\kappa_{Dj}X_j)\,dX_j \quad (2)$$

The following dimensionless groups are now defined for each sublayer:

$$\Phi_j(X_j, \kappa_{Dj}) = \frac{n_j^2 \sigma T_j^4(X_j, \kappa_{Dj}) - q_{o,j,s}}{q_{o,j,f} - q_{o,j,s}} \qquad (1 \le j \le J) \quad (3)$$

$$\Psi_j(\kappa_{Dj}) = \frac{q_r(\kappa_{Dj})}{q_{o,j,f} - q_{o,j,s}} \qquad (1 \le j \le J) \quad (4)$$

In terms of these quantities Eqs. (1) and (2) become

$$\Phi_j(X_j, \kappa_{Dj}) = \frac{1}{2} E_2(\kappa_{Dj} X_j) + \frac{1}{2} \kappa_{Dj} \int_0^1 \Phi_j(X_j^*, \kappa_{Dj}) \times E_1(\kappa_{Dj} |X_j - X_j^*|)\, dX_j^* \qquad (1 \le j \le J) \quad (5)$$

$$\Psi_j(\kappa_{Dj}) = 1 - 2\kappa_{Dj} \int_0^1 \Phi_j(X_j, \kappa_{Dj}) E_2(\kappa_{Dj} X_j)\, dX_j \qquad (1 \le j \le J) \quad (6)$$

Equations (5) and (6) are valid for each of the J sublayers. It is important to observe that Φ_j and Ψ_j are not functions of n_j. Hence, to obtain Φ_j and Ψ_j for all $n_j \ge 1$, it is necessary to solve Eq. (5) numerically, only once, for each value of the parameter κ_{Dj} and use each result to evaluate Eq. (6). This has already been done, and tabulated results for $\Phi(X, \kappa_D)$ and $\Psi(\kappa_D)$ from numerical solutions are in references such as Heaslet and Warming[15] and Siegel and Spuckler.[1,2]

Although the numerical solutions for $\Phi(X, \kappa_D)$ and $\Psi(\kappa_D)$ are available, the solutions required here for q_r through the composite layer, and for the $T_j(X_j)$ in each of the sublayers, have not yet been obtained. This is because Eqs. (3) and (4) contain unknown outgoing fluxes $q_{o,j,f}$, and $q_{o,j,s}$, at the first and second interfaces of each sublayer. These boundary fluxes for each of the j sublayers must be expressed in terms of known quantities. This is accomplished by looking in detail at the outer boundary and interior interface conditions.

At the two outer boundaries of the composite laminated layer, the internal fluxes leaving the internal interfaces of the first and Jth layers are related to the transmission of external flux from the surroundings and the reflection of incoming internal flux by

$$q_{o,1,f} = q_{r1}^o \tau_{1,f}^o + q_{i,1,f} \rho_{1,f}^i \quad (7a)$$

$$q_{o,J,s} = q_{r2}^o \tau_{J,s}^o + q_{i,J,s} \rho_{J,s}^i \quad (7b)$$

The superscripts o and i designate properties for radiation incident on the outside or inside of an interface. Thus $\tau_{j,f}^o$ is on the outside of the first interface of the jth sublayer as shown in Fig. 1b. At the inside surfaces of the two outer boundaries, the following relations exist between the radiative flux being transferred and the outgoing and incoming fluxes:

$$q_r = q_{o,1,f} - q_{i,1,f} \quad (8a)$$

$$q_r = -q_{o,J,s} + q_{i,J,s} \quad (8b)$$

Equations (7a) and (8a) are combined to eliminate $q_{i,1,f}$ and similarly Eqs. (7b) and (8b) are used to eliminate $q_{i,J,s}$. This yields

$$q_{o,1,f} = [1/(1 - \rho_{1,f}^i)](q_{r1}^o \tau_{1,f}^o - q_r \rho_{1,f}^i) \quad (9a)$$

$$q_{o,J,s} = [1/(1 - \rho_{J,s}^i)](q_{r2}^o \tau_{J,s}^o + q_r \rho_{J,s}^i) \quad (9b)$$

For the jth layer, at the first internal interface j, f, the two equations that involve reflected and transmitted fluxes are

$$q_r = q_{o,j,f} - q_{i,j,f}$$

$$q_{o,j,f} = q_{i,j-1,s} \tau_{j,f}^o + q_{i,j,f} \rho_{j,f}^i$$

The $q_{i,j,f}$ is eliminated to yield

$$q_{o,j,f} = [1/(1 - \rho_{j,f}^i)](q_{i,j-1,s} \tau_{j,f}^o - q_r \rho_{j,f}^i) \quad (10a)$$

At the second internal interface of the $j - 1$ layer, $j - 1, s$, the radiative flux is written in terms of incoming and outgoing fluxes as

$$q_r = q_{i,j-1,s} - q_{o,j-1,s}$$

This is used to eliminate $q_{i,j-1,s}$ from Eq. (10a) which gives the following relation between the outgoing fluxes and the radiant flux q_r being transferred:

$$q_{o,j,f} = [1/(1 - \rho_{j,f}^i)](q_{o,j-1,s} \tau_{j,f}^o - q_r \rho_{j,f}^i + q_r \tau_{j,f}^o) \quad (10b)$$

As a result of total reflections at interfaces when radiation passes into a medium with a lower refractive index, there are the following relations at the first and last internal interfaces of the entire layer and at the first internal surface of the jth sublayer[2,16]:

$$\tau_{1,f}^o = (1 - \rho_{1,f}^i) n_1^2 \quad (11a)$$

$$\tau_{J,s}^o = (1 - \rho_{J,s}^i) n_J^2 \quad (11b)$$

$$\tau_{j,f}^o = (1 - \rho_{j,f}^i)(n_j/n_{j-1})^2 \quad (11c)$$

Equation (11) is used to eliminate the τ from Eqs. (9) and (10b) to yield

$$q_{o,1,f} = n_1^2 q_{r1}^o - R_{1,f} q_r \quad (12a)$$

$$q_{o,J,s} = n_J^2 q_{r2}^o + R_{J,s} q_r \quad (12b)$$

$$q_{o,j,f} = (n_j/n_{j-1})^2 q_{o,j-1,s} - q_r [R_{j,f} - (n_j/n_{j-1})^2] \quad (12c)$$

where $R_j \equiv \rho_j^i/(1 - \rho_j^i)$. Equation (4) is now rearranged and used in Eqs. (12) to eliminate the $q_{o,j,s}$ fluxes at the second interface of each sublayer. This yields a set of simultaneous equations in terms of the $q_{o,j,f}$ fluxes at the first interfaces, the radiative flux q_r and the Ψ_j function. These equations are arranged into the following array:

$$\begin{aligned}
\frac{q_{o,1,f}}{n_1^2} &= q_{r1}^o - q_r \frac{R_{1,f}}{n_1^2} \\
\frac{q_{o,2,f}}{n_2^2} &= -q_r \left[\frac{R_{2,f}}{n_2^2} - \frac{1}{n_1^2} \left(1 - \frac{1}{\Psi_1} \right) \right] + \frac{q_{o,1,f}}{n_1^2} \\
&\vdots \\
\frac{q_{o,j,f}}{n_j^2} &= -q_r \left[\frac{R_{j,f}}{n_j^2} - \frac{1}{n_{j-1}^2} \left(1 - \frac{1}{\Psi_{j-1}} \right) \right] + \frac{q_{o,j-1,f}}{n_{j-1}^2} \\
&\vdots \\
\frac{q_{o,J,f}}{n_J^2} &= -q_r \left[\frac{R_{J,f}}{n_J^2} - \frac{1}{n_{J-1}^2} \left(1 - \frac{1}{\Psi_{J-1}} \right) \right] + \frac{q_{o,J-1,f}}{n_{J-1}^2} \\
-\frac{q_{o,J,f}}{n_J^2} &= -q_{r2}^o - \frac{q_r}{n_J^2} \left(R_{J,s} + \frac{1}{\Psi_J} \right)
\end{aligned} \quad (13)$$

The equations in (13) are now added, which eliminates all of the q_o terms; this yields the equation for the radiative flux q_r, as

$$\frac{q_r}{q^o_{r1} - q^o_{r2}} = \bar{q}_r = \frac{1}{\frac{R_{1,f}}{n_1^2} + \sum_{j=2}^{J}\left(\frac{R_{j,f}}{n_j^2} - \frac{1}{n_{j-1}^2}\right) + \frac{R_{J,s}}{n_J^2} + \sum_{j=1}^{J}\frac{1}{n_j^2\Psi_j}} \tag{14}$$

The temperature distributions in the individual sublayers are now obtained. Using the set of Eqs. (13), the first j equations are added to obtain

$$\frac{q_{o,j,f} - n_j^2 q^o_{r1}}{n_j^2 q_r} + \left\{\frac{R_{1,f}}{n_1^2} + \sum_{k=2}^{j}\left[\frac{R_{k,f}}{n_k^2} - \frac{1}{n_{k-1}^2}\left(1 - \frac{1}{\Psi_{k-1}}\right)\right]\right\} = 0 \tag{15}$$

The desired temperature distribution $T_j(X_j)$ is now written in terms of a dimensionless function $\bar{T}_j^4(X_j)$ as

$$\bar{T}_j^4 = \frac{\sigma T_j^4 - q^o_{r2}}{q^o_{r1} - q^o_{r2}} = \frac{n_j^2\sigma T_j^4 - n_j^2 q^o_{r2}}{q_r}\frac{q_r}{n_j^2(q^o_{r1} - q^o_{r2})} = \frac{q_r}{q^o_{r1} - q^o_{r2}}\left(\frac{n_j^2\sigma T_j^4 - q_{o,j,s}}{n_j^2 q_r} + \frac{q_{o,j,s} - n_j^2 q^o_{r2}}{n_j^2 q_r}\right) \tag{16}$$

The ratio of Eqs. (3) and (4) is substituted into the first term in parentheses of Eq. (16) to obtain

$$\bar{T}_j^4 = \frac{q_r}{q^o_{r1} - q^o_{r2}}\left(\frac{\Phi_j}{n_j^2\Psi_j} + \frac{q_{o,j,s} - n_j^2 q^o_{r2}}{n_j^2 q_r}\right) \tag{17}$$

The negative of Eq. (15) is now inserted into the parentheses on the right side of Eq. (17). After rearrangement and using Eq. (4), the result for the temperature distribution (in terms of the dimensionless function $\bar{T}_j^4$) of the jth sublayer is

$$\bar{T}_j^4 = 1 - \frac{q_r}{q^o_{r1} - q^o_{r2}}\left\{\frac{1 - \Phi_j}{n_j^2\Psi_j} + \frac{R_{1,f}}{n_1^2} + \sum_{k=2}^{j}\left[\frac{R_{k,f}}{n_k^2} - \frac{1}{n_{k-1}^2}\left(1 - \frac{1}{\Psi_{k-1}}\right)\right]\right\} \qquad (1 < j < J) \tag{18a}$$

The first and last sublayers are special cases, and by similar manipulations their dimensionless temperature function distributions are obtained from

$$\bar{T}_1^4 = 1 - \frac{q_r}{q^o_{r1} - q^o_{r2}}\left(\frac{R_{1,f}}{n_1^2} + \frac{1 - \Phi_1}{n_1^2\Psi_1}\right) \tag{18b}$$

$$\bar{T}_J^4 = \frac{q_r}{q^o_{r1} - q^o_{r2}}\left(\frac{R_{J,s}}{n_J^2} + \frac{\Phi_J}{n_J^2\Psi_J}\right) \tag{18c}$$

The temperature distributions in all the layers can therefore be evaluated from Eqs. (18) after the dimensionless radiative flux $q_r/(q^o_{r1} - q^o_{r2})$ has been obtained from Eq. (14).

To use these relations, the internal interface reflectivity ρ_j^i values are needed to evaluate the R_j for various refractive indices of the sublayers. In the absence of better information, the following relations are used. The externally incident radiation is diffuse, and as a result of internal scattering and diffuse emission it is assumed that the internal radiation is also diffuse at the interfaces. Although the interfaces are not optically smooth, it is assumed that each bit of roughness acts as a smooth facet so that the reflectivity can be obtained from the Fresnel interface relations for a dielectric medium. The reflected energy integrated over all incident directions for a diffuse incident distribution gives the relation for $\rho^i(n)$[14]

$$\rho^i(n) \equiv F(n) = \frac{1}{2} + \frac{(3n + 1)(n - 1)}{6(n + 1)^2} + \frac{n^2(n^2 - 1)^2}{(n^2 + 1)^3}\mathcal{L}_n\left(\frac{n - 1}{n + 1}\right) - \frac{2n^3(n^2 + 2n - 1)}{(n^2 + 1)(n^4 - 1)} + \frac{8n^4(n^4 + 1)}{(n^2 + 1)(n^4 - 1)^2}\mathcal{L}_n(n) \tag{19a}$$

This is for diffuse radiation incident on a material with a higher refractive index, where $n = n_H/n_L$ (n_H and n_L are the "higher" and "lower" n values). When diffuse radiation is traveling in the reverse direction from a higher to a lower n value material, ρ^i is given by[16]

$$\rho^i(n) = 1 - (1/n^2)[1 - F(n)] \qquad (n = n_H/n_L) \tag{19b}$$

The reflectivity relations in Eq. (19) are derived for surfaces of dielectrics in the limit of infinite electrical resistivity, and for this condition they do not attenuate radiation internally. As discussed by Cox,[17] in the spectral regions where ceramic materials are reasonably transparent to radiation, so that internal radiation will affect the temperature distribution, the extinction coefficient κ (not to be confused with its optical thickness) in the complex index of refraction ($n - i\kappa$) is usually not large enough to significantly affect the surface reflectivity. Hence, Eq. (19) for nonattenuating dielectrics often provides reasonable reflectivity results for attenuating dielectrics. The absorption coefficient a in a material, is related to its extinction coefficient κ by $a = 4\pi\kappa/\lambda_o$. Since wavelengths for thermal radiation are in the micrometer range, only a small value of κ is required to yield a large value for a. If κ is large enough to influence the interface reflectivity relations, $a = 4\pi\kappa/\lambda_o$ will be so large that the radiating layer is essentially opaque, unless its thickness is much smaller than the ceramic layers considered here.

The Φ and Ψ are the building blocks to evaluate the present solution for a laminated composite layer that includes refractive index effects and interface reflections. To evaluate results from Eqs. (14) and (18), the exact functions $\Phi(X, \kappa_D)$ and $\Psi(\kappa_D)$ can be used as obtained from numerical solutions of Eqs. (1) and (2); these functions are available in the literature as referenced earlier. Exact functions from the numerical integration are tabulated in Siegel and Spuckler[1] for optical thicknesses, $0.1 \leq \kappa_D \leq 100$. A convenient alternative to use for the functions $\Phi(X, \kappa_D)$ and $\Psi(\kappa_D)$ are the diffusion solution results which have the advantage of being simple analytical expressions. The use of these approximate functions to build up solutions was found to give accurate results for a two-layer composite.[2] The diffusion functions for a plane layer are given by[14]

$$\Psi(\kappa_D) = [1/(\tfrac{3}{4}\kappa_D + 1)] \tag{20a}$$

$$\Phi(X, \kappa_D) = \Psi(\kappa_D)[\tfrac{3}{4}\kappa_D(1 - X) + \tfrac{1}{2}] \tag{20b}$$

Very good comparisons were obtained for the present results evaluated by using both the exact and the diffusion functions for $\Phi(X, \kappa_D)$ and $\Psi(\kappa_D)$. For this reason, and because tabular results for the exact solution are limited, the diffusion solution is recommended for simplicity and sufficient accuracy for heat flux and temperature distribution calculations using the present analytical equations. When used in Eqs. (14) and (18), Eqs. (20) provide rapid predictions of heat flux and temperature distributions for any refractive indices and optical thicknesses of the individual sublayers in the laminate. For the graphical results shown here, $\Phi(X, \kappa_D)$ and $\Psi(\kappa_D)$ were obtained from Eqs. (20), but the exact functions in Ref.

1 can also be used to yield similar results as shown on one of the figures.

Results and Discussion

Effect of Variation of Refractive Index

Figure 2 shows the effect on the dimensionless temperature function of having the refractive index increase across the thickness of a plane layer. In Fig. 2a, the refractive index increases from one to three in equal increments within the five sublayers comprising the total thickness; in Fig. 2b the number of sublayers is increased to 21 to provide a more continuous variation of n over the same range of n. A large n increases the local internal radiation emission which is proportional to n^2 for a gray material. A larger refractive index in a material relative to its surroundings also increases the amount of internal reflection at its bounding interfaces. This is the result of total internal reflection when radiation is directed out of a material with a higher refractive index. These effects of refractive index act to distribute energy across a layer by virtue of emission and internal reflections. As a result, in Fig. 2 the temperature profiles become more uniform as the n value increases across the layer thickness.

Effect of Total Optical Thickness

Figure 2 also shows the effect of the total optical thickness of the layer. For this figure, the optical thicknesses of each of the sublayers are all equal so that for each value of κ_D, $\kappa_{Dj} = \kappa_D/J$, where J is the total number of layers. When $\kappa_D = 0.1$, the optical thickness of each sublayer is small enough so that the temperature in each sublayer is almost uniform, as is characteristic of an optically thin region. There are temperature jumps between layers. These temperature discontinuities occur at interfaces that separate regions of different refractive indices when heat transfer is only by radiation (the limiting condition analyzed here). The presence of heat conduction would eliminate the temperature discontinuities at the interfaces, but there can be large local temperature gradients near the interfaces if conduction is small, relative to radiation. As shown in Fig. 2, the discontinuities decrease as the optical thickness increases. For $\kappa_D = 100$, the temperature profile in Fig. 2b is essentially continuous.

As optical thickness increases, the resistance to radiative heat flow increases, so that the temperature gradients increase throughout the entire layer and within each sublayer. For $\kappa_D = 0.1$ the layer is optically thin, and the change in the dimensionless temperature function across the entire layer is only about 0.25. For $\kappa_D = 100$, however, the range in the temperature function increases to about 0.95. The dimensionless radiative heat fluxes (given in the figure legend) illustrate how the heat flux decreases as the optical thickness is increased. Making n more continuous by increasing the number of sublayers increased q_r slightly.

Effect of Increasing and Decreasing Refractive Indices in a Layer

For the distributions in Fig. 2, the refractive index increased in uniform increments across the entire composite layer. Figure 3a shows the effect of a uniform incremental increase from $n = 1$ in the first layer to $n = 3$ in the central two

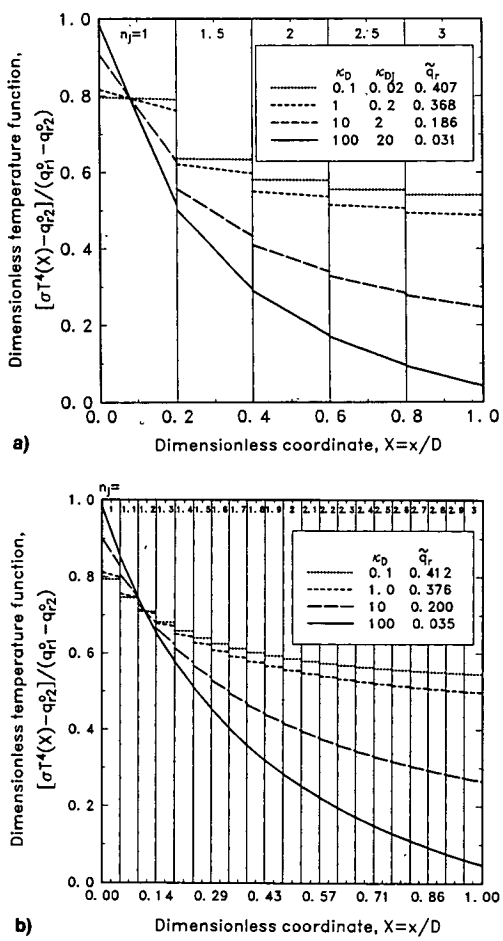

Fig. 2 Dimensionless temperature distributions in a composite region with the index of refraction increasing from one to three through the total thickness. The total optical thicknesses are $\kappa_D = 0.1, 1, 10, 100$, and the sublayers have equal thicknesses so that $\kappa_{Dj} = \kappa_D/J$: a) number of layers, $J = 5$; b) number of layers, $J = 21$.

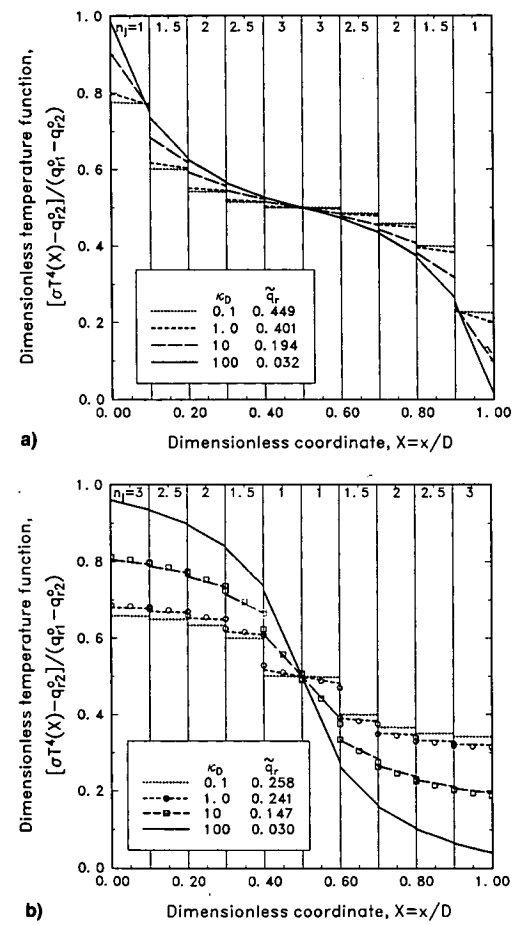

Fig. 3 Dimensionless temperature distributions in a 10-layer composite region with the index of refraction varying in the range from one to three. The total optical thicknesses are $\kappa_D = 0.1, 1, 10, 100$, and the sublayers have equal thicknesses so that $\kappa_{Dj} = \kappa_D/10$: a) refractive index increases from one to three and then decreases to one; b) refractive index decreases from three to one and then increases to three; symbols show solution using exact Ψ and Φ functions, dashed lines are results using diffusion relations for Ψ and Φ.

sublayers, and then a uniform incremental decrease to reach $n = 1$ in the final sublayer. The optical thicknesses of the sublayers are all equal so that for each sublayer $\kappa_{Dj} = \kappa_D/J$, where $J = 10$. The same total optical thicknesses are used as in Fig. 2, $\kappa_D = 0.1, 1, 10, 100$. In Figs. 3a and 3b there is the same portion of the total layer thickness at each of the refractive indices, as in Fig. 2a. Each of the sublayers in Fig. 2a has been divided in half and the order of the resulting 10 layers rearranged. Thus, useful comparisons can be made between Figs. 3a and 2a. In Fig. 3a the dimensionless temperature distributions become flat in the central portion of the layer where the refractive index is largest. The profiles are asymmetric about the center plane. The effect of increasing the optical thickness on the temperature distribution through the entire laminate is not as pronounced as in Fig. 2. Comparing the heat fluxes in Figs. 3a and 2a shows the rearrangement of the layers to begin and end with the same index as the surroundings has resulted in a small increase in q_r.

Effect of Order of Refractive Indices in Heat Flow Direction

In Fig. 3b the κ_D values are the same as in Fig. 3a. The n values, however, are interchanged so that the largest refractive index, $n = 3$, is now adjacent to each of the two outer boundaries. Then proceeding toward the center, the n decreases in uniform increments to one, such that the n variation is symmetric across the entire layer. As compared with Fig. 3a, the different distribution of n values changes the distribution of totally reflected energy within the sublayers. There is also partial reflection of the incident flux q^+_{r1}; this did not occur for the conditions in Fig. 3a where $n = 1$ in the outermost sublayers, and therefore, matches the n of the surroundings. The dimensionless temperature function distributions have their largest gradients in the center of the layer where n has its lowest value. Compared with Fig. 3a, the variation of κ_D has a larger effect. The profiles are again asymmetric about the center plane. For small κ_D, there is a significant reduction in the radiative flux being transferred, compared to Figs. 2 and 3a.

Figure 3b also provides a comparison with solutions computed using the exact functions for $\Phi(X, \kappa_D)$ and $\Psi(\kappa_D)$; the exact solutions are plotted for two values of κ_D using square and circular symbols to make them distinct from the dashed lines that were obtained using the diffusion functions. The comparisons are excellent showing the validity of using the very convenient diffusion relations for these basic functions.

Reciprocal Behavior of Dimensionless Temperatures

Figure 4 illustrates a general reciprocal behavior for the temperature results; an example with five sublayers is used. The reciprocal behavior is valid for an arbitrary number of layers and for a continuous variation in n. In Fig. 4a, the n increases linearly in an incremental fashion from one to three progressing from the hot to the cold side. Rather than having equal κ_{Dj} as in Figs. 2 and 3, the κ_{Dj} have various values to illustrate the nature of κ_{Dj} variations. The physical thicknesses of the sublayers is shown as equal, but they could be unequal, as the solution depends only on the optical thicknesses κ_{Dj} (this will be discussed in Fig. 4c). In Fig. 4b, both the n values and the optical thicknesses of the five layers are reversed in their order, relative to the hot side as compared to Fig. 4a. The reciprocal result obtained is that rotating Fig. 4a by 180 deg gives the same dimensionless temperature distributions as in Fig. 4b. It was also found that the radiative heat flux through the laminate is independent of reversing the order of the multiple layers relative to the side with larger incident radiation; hence, in Fig. 4b, the heat fluxes remain the same as in Fig. 4a.

Although the radiative behavior depends on the κ_{Dj}, rather than the physical thicknesses D_j of the layers, the temperature gradients depend on the D_j. As an illustration, the solution in Fig. 4a is given in Fig. 4c, with three of the sublayers having small physical thicknesses as might be characteristic of reinforcing layers in a ceramic material or a coated part. The temperature variation through each sublayer remains the same, but in a sublayer with a smaller physical thickness, the local gradient of the dimensionless temperature function is increased.

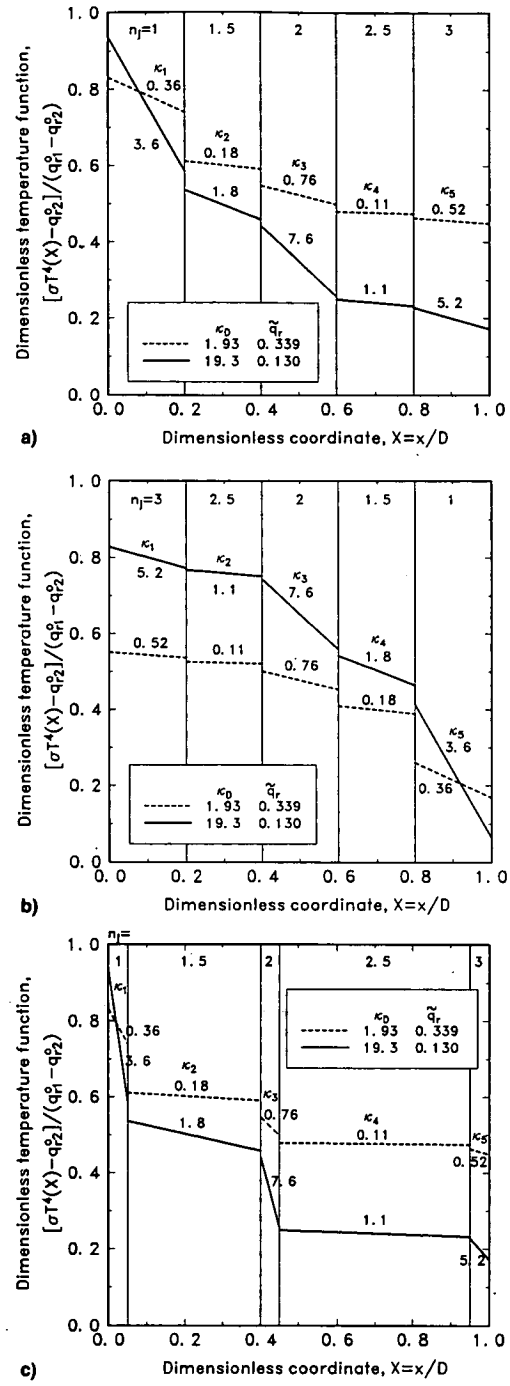

Fig. 4 Dimensionless temperature distributions in a five – layer composite region with the index of refraction increasing from one to three through the total thickness. The effect is shown of having different optical thicknesses for each sublayer. Total optical thickness are κ_D = 1.93 and 19.3: a) refractive index increases from one to three for various κ_{Dj}; b) variations in both n_j and κ_{Dj} are reversed compared with part a; and c) part a with layers having unequal physical thicknesses.

Figure 5 shows the effect of having different rates of increase of the index of refraction within a layer. Consider the three solid curves; they are all for a total optical thickness of $\kappa_D = 100$. As shown in the legend, the three thicknesses of the solid lines correspond to different increases in the refractive index within the layer. For the curve drawn with a thin

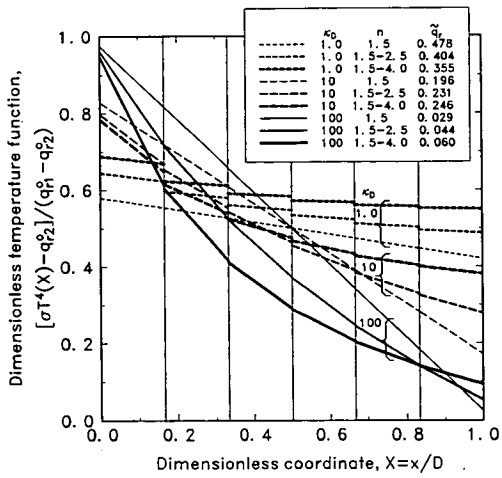

Fig. 5 Effect of the rate of increase of the refractive index within the layer for various optical thicknesses.

line, $n = 1.5$ throughout the layer. For the curve with a medium thickness line, n increases in a stepwise fashion of $\Delta n_j = 0.2$ for each sublayer, so the first and final sublayers have $n = 1.5$ and 2.5. For the heaviest line, $\Delta n_j = 0.5$, so that n has the range 1.5–4.0 across the layer. Increasing the n variation results in increased curvature of the dimensionless temperature function. For $\kappa_D = 10$ there are the same trends, this is shown by the three curves drawn with the longer dashes. The remaining three curves drawn with the short dashes are for a smaller optical thickness, $\kappa_D = 1$. In this instance it was found that the curves do not cross and the temperatures increase as Δn becomes larger.

The dimensionless radiative heat flux also has different trends as the optical thickness changes from 1 to 100. For $\kappa_D = 1$, the radiative flux decreases as the gradient in refractive index increases (larger Δn_j). For an optically thick layer, the behavior is reversed and a greater increase of n with x increases the radiant energy transfer.

Conclusions

A method was developed for obtaining temperature distributions and radiative heat fluxes in a plane layer with an index of refraction and optical density that varies within its thickness. The approach that was derived is to analyze a laminated region with many layers that can each have a different refractive index and optical thickness. The interfaces between layers are assumed diffuse with the intent of providing information on the limiting case of energy transfer only by radiation in a ceramic material with layers having various compositions. Radiative energy is incident on each outer boundary. The multilayer laminate is in radiative equilibrium (limiting case of zero heat conduction) and emits, absorbs, and isotropically scatters radiation. The method yields results for multiple laminated layers with arbitrary indices of refraction by using the known dimensionless temperature and heat flux functions for a single semitransparent radiating layer with $n = 1$. These functions are combined through the coupling at the interfaces to build up solutions for a multilayer laminated region. The coupling relations include transmission through the interfaces and all internal reflections within the layers. The result is a set of simple algebraic expressions for the temperature distribution in each of the sublayers and for the radiative heat flux through the laminated composite region. Sample results were evaluated using the basic functions for a single layer with $n = 1$ obtained by exact numerical integration and by diffusion methods. The results using diffusion functions were found to be within engineering accuracy. Using these functions provides an especially simple way for computing multilayer results for any distribution of optical thickness.

Illustrative dimensionless temperature function distributions and radiative fluxes are given for a variety of refractive index variations and optical thicknesses of the layers. A reciprocity relation was found for the temperature function distributions. If the order of the indices of refraction of the sublayers is reversed as well as their optical thicknesses, the temperature distributions become inverted mirror images while the radiative heat flux is unchanged. It was found that increasing the local refractive index in a layer makes the local temperature distribution more uniform by means of increased internal reflection of energy. The effect that this has on the radiative energy transfer depends on the optical thickness of the composite.

References

[1]Siegel, R., and Spuckler, C. M., "Effect of Index of Refraction on Radiation Characteristics in a Heated Absorbing, Emitting and Scattering Layer," *Journal of Heat Transfer*, Vol. 114, No. 3, 1992, pp. 781–784.

[2]Siegel, R., and Spuckler, C. M., "Refractive Index Effects on Radiation in an Absorbing, Emitting and Scattering Laminated Layer," *Journal of Heat Transfer* (to be published).

[3]Gardon, R., "Calculation of Temperature Distributions in Glass Plates Undergoing Heat-Treatment," *Journal of the American Ceramic Society*, Vol. 41, No. 6, 1958, pp. 200–209.

[4]Fowle, A. A., Strong, P. F., Comstock, D. F., and Sox, C., "Computer Program to Predict Heat Transfer Through Glass," *AIAA Journal*, Vol. 7, No. 3, 1969, pp. 478–483.

[5]Rokhsaz, F., and Dougherty, R. L., "Radiative Transfer Within a Finite Plane-Parallel Medium Exhibiting Fresnel Reflection at a Boundary," *Heat Transfer Phenomena in Radiation, Combustion and Fires*, American Society of Mechanical Engineers, HTD-Vol. 106, Aug. 1989, pp. 1–8.

[6]Ping, T. H., and Lallemand, M., "Transient Radiative-Conductive Heat Transfer in Flat Glasses Submitted to Temperature, Flux, and Mixed Boundary Conditions," *International Journal of Heat and Mass Transfer*, Vol. 32, No. 5, 1989, pp. 795–810.

[7]Crosbie, A. L., and Shieh, S. M., "Three-Dimensional Radiative Transfer for Anisotropic Scattering Medium with Refractive Index Greater than Unity," *Journal of Quantitative Spectroscopy and Radiative Transfer*, Vol. 44, No. 2, 1990, pp. 299–312.

[8]Reguigui, N. M., and Dougherty, R. L., "Two-Dimensional Radiative Transfer in a Cylindrical Layered Medium with Reflecting Interfaces," *Journal of Thermophysics and Heat Transfer*, Vol. 6, No. 2, 1992, pp. 232–241.

[9]Amlin, D. W., and Korpela, S. A., "Influence of Thermal Radiation on the Temperature Distribution in a Semi-Transparent Solid," *Journal of Heat Transfer*, Vol. 101, No. 1, 1979, pp. 76–80.

[10]Tarshis, L. A., O'Hara, S., and Viskanta, R., "Heat Transfer by Simultaneous Conduction and Radiation for Two Absorbing Media in Intimate Contact," *International Journal of Heat and Mass Transfer*, Vol. 12, No. 3, 1969, pp. 333–347.

[11]Thomas, J. R., Jr., "Coupled Radiation/Conduction Heat Transfer in Ceramic Liners for Diesel Engines," *Numerical Heat Transfer*, Pt. A, Vol. 21, 1992, pp. 109–120.

[12]Ritchie, I. T., and Window, B., "Applications of Thin Graded-Index Films to Solar Absorbers," *Applied Optics*, Vol. 16, No. 5, 1977, pp. 1438–1443.

[13]Snail, K. A., "Analytical Solutions for the Reflectivity of Homogeneous and Graded Selective Absorbers," *Solar Energy Materials*, Vol. 12, No. 6, 1985, pp. 411–424.

[14]Siegel, R., and Howell, J. R., *Thermal Radiation Heat Transfer*, 3rd ed., Hemisphere, Washington, DC, 1992.

[15]Heaslet, M. A., and Warming, R. F., "Radiative Transport and Wall Temperature Slip in an Absorbing Planar Medium," *International Journal of Heat and Mass Transfer*, Vol. 8, No. 7, 1965, pp. 979–994.

[16]Richmond, J. C., "Relation of Emittance to Other Optical Properties," *Journal of Research of the National Bureau of Standards*, Vol. 67C, No. 3, 1963, pp. 217–226.

[17]Cox, R. L., "Fundamentals of Thermal Radiation in Ceramic Materials," *Thermal Radiation in Solids*, edited by S. Katzoff, NASA SP-55, 1965, pp. 83–101.